第 33 卷第 12 期 无 机 化 学 学 报 Vol.33 No.12
2017 年 12 月 CHINESE JOURNAL OF INORGANIC CHEMISTRY 2287-2295

两个 dpa 类配体的铜(Ⅱ)配合物的合成、结构、核酸酶活性及细胞毒性

岳爱琴[1] 张宇婷[2] 张鹏骞[3] 高媛媛[4] 张永坡[2]
王 敏[1] 高春艳*,[2] 赵晋忠[2] 杜维俊*,[1]
([1]山西农业大学农学院,太谷 030801)
([2]山西农业大学文理学院,太谷 030801)
([3]北京麋鹿生态实验中心,北京 100076)
([4]内蒙古工业大学化工学院,呼和浩特 010051)

摘要:以 dpa 衍生配体 4-methyl-*N*,*N*-bis(pyridin-2-ylmethyl)aniline(L)合成 2 个单核铜配合物[CuL(NO_3)$_2$] (**1**)和[CuL(OAc)(H_2O)]ClO_4 (**2**),并对其进行了表征。单晶结构显示,配合物 **1** 中的 Cu 中心可以描述为畸变的五角双锥构型,而 **2** 的 Cu 中心为畸变的八面体构型。运用电子吸收和发射光谱法研究了配合物与 CT-DNA 的键合作用,结果表明 2 个配合物与 DNA 的相互作用均为部分插入模式。通过改变浓度、时间进一步检测配合物切割 DNA 的能力,以及验证其切割机理,结果表明在外界诱导剂存在下,2 个配合物均表现出强的切割 DNA 的能力,其作用机理为氧化切割机理,其中活性氧可能为·OH 和 $^1O_2$。利用 MTT 法测定了配合物对体外 HeLa、HepG-2 和 SGC-7901 肿瘤细胞增殖的抑制能力。

关键词:铜配合物;dpa 类配体;DNA 键合;DNA 切割;细胞毒性
中图分类号:O614.121 **文献标识码**:A **文章编号**:1001-4861(2017)12-2287-09
DOI:10.11862/CJIC.2017.273

Two Copper(Ⅱ) Complexes with dpa-Based Ligand: Syntheses, Structures, Nuclease Activity and Cytotoxicity

YUE Ai-Qin[1] ZHANG Yu-Ting[2] ZHANG Peng-Qian[3] GAO Yuan-Yuan[4] ZHANG Yong-Po[2]
WANG Min[1] GAO Chun-Yan*,[2] ZHAO Jin-Zhong[2] DU Wei-Jun*,[1]
([1]*College of Agronomy, Shanxi Agricultural University, Taigu, Shanxi* 030801, *China*)
([2]*College of Arts and Sciences, Shanxi Agricultural University, Taigu, Shanxi* 030801, *China*)
([3]*Beijing Milu Ecological Research Center, Beijing* 100076, *China*)
([4]*Chemical Engineering College, Inner Mongolia University of Technology, Hohhot* 010051, *China*)

Abstract: Two new mononuclear copper(Ⅱ) complexes, [CuL(NO_3)$_2$] (**1**) and [CuL(OAc)(H_2O)]ClO_4 (**2**), with dpa-based ligand (L=4-methyl-*N*,*N*-bis(pyridin-2-ylmethyl)aniline) have been synthesized and characterized by various physico-chemical techniques. The crystal structure of complex **1** displays a distorted pentagonal bipyramidal geometry, and the geometry around copper center of **2** can be described as a distorted octahedron. Interaction of the complexes with CT-DNA has been explored by using absorption and emission spectral methods, and the result suggests that the binding strength of the two complexes with DNA is a medium intercalative mode. The

收稿日期:2017-05-15。收修改稿日期:2017-09-28。
国家自然科学基金(No.31171580)、山西省高等学校科技创新项目(No.2015148)、山西省自然科学基金(No.201601D011076,201701D221157)、山西省重点研发计划项目(No.201703D221008-4,201703D221004-5)、山西农业大学中青年拔尖创新人才支持计划(No.201203)、山西农业大学引进人才科研启动金(No.2013YJ40)、山西省煤基重点项目(No.FT201402-01)、内蒙古自然科学基金(No.2016BS0206)和内蒙古自治区高等学校科学研究项目(No.NJZY088)。
*通信联系人。E-mail:gaocynk@163.com,duweijun68@126.com;会员登记号:S06N2534M1605。

concentration-dependent and time-dependent DNA cleavage activity and the mechanism of DNA cleavage have been investigated, which suggest the DNA cleavage efficiencies of both complexes exhibit remarkable enhancement in the presence of external revulsants, and oxidative mechanism has been demonstrated via the pathway involving both hydroxyl radicals (·OH) and singlet oxygen ($^1O_2$) as ROS. The *in vitro* cytotoxic activity of the complexes has been examined by MTT on three cell lines such as HeLa, HepG-2 and SGC-7901. CCDC: 1521098, **1**; 1521097, **2**.

Keywords: copper(Ⅱ) complexes; dpa-based ligand; DNA binding; DNA cleavage; cytotoxicity

0 Introduction

Medicinal inorganic chemistry has been a research field of broad interest since the discovery of cisplatin as well as its anticancer activity in the 1960s[1-3]. For the reason of severe side effects, general toxicity and drug resistance problems of cisplatin and its derivatives, metal-based therapeutics is a still expanding field up to now that has not stopped at the point of the discovery of new anticancer drug[4-5]. Besides platinum, candidates of complexes for almost all transition metals are investigated in the past few years[6-8] for the purpose of developing new anticancer drugs with more efficient and less systemic toxicity. Among those transition metal compounds, copper complex is an interesting candidate showing much potential over cisplatin and its derivatives of reduced toxicity, novel action mechanism, various activity spectrum, and non-cross-resistance prospect[9].

Besides the choice of metal ions, purposeful design of ligand framework can significantly alter the biological properties by limiting the adverse effects of metal ion overload, modifying reactivity and lipophilicity, stabilizing specific oxidation states, and facilitating metal ion redistribution[10]. Polypyridyl metal complexes have been exploited in a broad range of biological applications for their polydentate chelating structure and unique chemical and redox properties[11]. In our previous works, we have reported the biological activity of Ni(Ⅱ)[12] and Zn(Ⅱ)[13-14] complexes containing polypyridyl ligands, the results suggested the complexes performed considerable cytotoxic activities. As a continuation of our interest, in this work, two new copper complexes with a mononuclear polypyridyl ligand were synthesized and structurally characterized. The DNA cleavage efficiencies and the cytotoxicity of the two complexes have been tested and analyzed.

1 Experimental

1.1 Materials and method

The reagents and solvents were purchased from commercial sources. Tridentate dpa-based ligand 4-methyl-*N*,*N*-bis (pyridin-2-ylmethyl)aniline (L) and L·xHClO$_4$ was synthesized according to previous work[12,14]. Calf thymus (CT-DNA), Plasmid pBR322 DNA and ethidium bromide (EB) were purchased from Sigma-Aldrich. Stock solutions of Cu(Ⅱ) complexes (1.0 mmol·L^{-1} in 10%(*V*/*V*) DMF aqueous solution) were stored at 4 ℃ and prepared to series concentrations for all experiments. Tris-HCl was prepared using triple-distilled deionized sonicated water.

Elemental analyses and IR spectra were obtained on the Perkin-Elmer analyzer and Perkin-Elmer FT-IR spectrometer, respectively. Electronic spectra and fluorescence spectral data were collected on the JASCO V-570 spectrophotometer and MPF-4 fluorescence spectrophotometer at room temperature. The gel imaging and documentation DigiDoc-It System were assessed using Labworks Imaging and Analysis Software (UVI, England). The MTT assay was determined by measuring the absorbance of each well at 570 nm using a Bio-Rad 680 microplate reader (Bio-Rad, USA).

1.2 Preparation of the complexes

1.2.1 Synthesis of [CuL(NO$_3$)$_2$] (**1**)

A methanol solution (10 mL) with 0.2 mmol L·xHClO$_4$ (x was counted as 1) was added to the ethanol solution (10 mL) of Cu(NO$_3$)$_2$·3H$_2$O (0.2 mmol, 48 mg).

The resulting mixture was stirred for 10 h at room temperature. After filtration, green prism crystals suitable for X-ray diffraction were obtained by slow evaporation of the filtrate after a week, which were collected by filtration, washed with diethyl ether and dried in air (Yield: 45%). Anal. Calcd. for $C_{19}H_{19}CuN_5O_6$ (%): C, 47.85; H, 4.02; N, 14.68. Found(%): C, 48.32; H, 3.29; N, 14.76. FT-IR (KBr, cm^{-1}): 3 445, 2 924, 2 362, 1 613, 1 516, 1 475, 1 386, 1 294, 1 120, 1 031, 818, 782, 624.

1.2.2　Synthesis of $[CuL(OAc)(H_2O)]ClO_4$ (**2**)

Complex **2** was prepared using a similar procedure with that of **1** except of adding an aqueous solution (5 mL) of $Cu(OAc)_2\cdot H_2O$ (0.2 mmol, 40 mg) to the reaction mixture. Blue prism crystals suitable for X-ray diffraction were precipitated by slow evaporation of the filtrate after a week, which were collected by filtration, washed with cold diethyl ether and dried in vacuum (yield: 42%). Anal. Calcd. for $C_{21}H_{24}ClCuN_3O_7$ (%): C, 47.64; H, 4.57; N, 7.94. Found(%): C, 47.71; H, 4.63; N, 7.85. FT-IR (KBr, cm^{-1}): 3 490, 1 582, 1 512, 1 400, 1 342, 1 286, 1 099, 972, 929, 832, 773, 929, 832, 773, 687, 624, 560, 421.

1.3　X-ray crystallography

Single crystals of the complexes with suitable size (0.40 mm×0.25 mm×0.12 mm for **1** and **2**) were selected. X-ray diffraction data were collected on a Bruker Smart 1000 CCD diffractometer using Mo $K\alpha$ radiation (λ=0.071 073 nm) with the ω-2θ scan technique. Diffraction data were collected at 293(2) K. Both the crystal structures were solved using direct methods (SHELXS-97)[15] and refined with full-matrix least-squares technique on F^2 using the SHELXL-97[16]. The hydrogen atoms were added theoretically, and riding on the concerned atoms and refined with fixed thermal factors. Crystallographic data details and structure refinement parameters are presented in Table 1. Selected bond lengths and angles are listed in Table S1.

CCDC: 1521098 for **1**; 1521097 for **2**.

Table 1　Crystallographic data for complexes 1 and 2

Complex	1	2
Empirical formula	$C_{19}H_{19}CuN_5O_6$	$C_{21}H_{24}ClCuN_3O_7$
Formula weight	476.91	529.42
Crystal system	Triclinic	Monoclinic
Space group	$P\bar{1}$	$P2_1/c$
a / nm	0.799 90(16)	0.885 90(18)
b / nm	0.874 40(17)	1.311 9(3)
c / nm	1.730 4(3)	2.061 0(4)
α / (°)	75.90(3)	90
β / (°)	85.12(3)	92.89(3)
γ / (°)	66.03(3)	90
V / nm^3	1.072 5(4)	2.392 3(9)
Z	2	4
D_c / ($g\cdot cm^{-3}$)	1.477	1.470
F(000)	490	1 092
θ range for data collection / (°)	2.99~25.01	2.99~25.01
Limiting indices (h, k, l)	$-9 \leqslant h \leqslant 9, -10 \leqslant k \leqslant 10, -20 \leqslant l \leqslant 20$	$-10 \leqslant h \leqslant 10, -15 \leqslant k \leqslant 15, -24 \leqslant l \leqslant 22$
Reflections collected	6 124	13 585
Independent reflections (R_{int})	3 699 (0.048 9)	4 208 (0.032 7)
Goodness-of-fit on F^2	1.014	1.094
R_1, wR_2 [$I>2\sigma(I)$]	R_1=0.104 4, wR_2=0.267 4	R_1=0.049 3, wR_2=0.117 5
R_1, wR_2 (all data)	R_1=0.124 5, wR_2=0.288 3	R_1=0.060 2, wR_2=0.123 1
$(\Delta\rho)_{max}$, $(\Delta\rho)_{min}$ / ($e\cdot nm^{-3}$)	1 532, −2 286	575, −538

1.4 DNA binding, DNA cleavage and cytotoxicity experiments

The chemical nuclease activity and cytotoxicity experiments were conducted using the similar methods described previously[12-14,17]. Detailed experimental methods can be found in the supporting information.

2 Results and discussion

2.1 Description of the crystal structures

Both of the mononuclear Cu(Ⅱ) complexes have been structurally characterized by X-ray crystallography (Fig.1). Complex **1** crystallizes in a triclinic cell with $P\bar{1}$ space group. The metal center is hepta-coordinated with N_3O_4 donor sets, and weak coordinated interactions (Cu1-O2 0.257 5(5) nm and Cu1-O4 0.247 4(5) nm) exist in the $[CuL(NO_3)_2]$ unit. The atoms O1, O2, N1, O4 and O6 occupy the corners of the pentagonal basal plane, and the angles around the copper ion within the basal plane vary from 46.28(7)° to 99.04(13)° and the sum of angles spanning these five bonds is 360.07° (Table S1), underscoring the flat nature of this equatorial plane. In addition, the atoms N2 and N3 occupy the axial positions (Cu1-N2 0.195 1(7) nm; Cu1-N3 0.195 9 (6) nm and N2-Cu1-N3 164.7 (3)°). Therefore, the geometry around copper center can be described as a distorted pentagonal bipyramidal.

Complex **2** crystallizes in a monoclinic cell with $P2_1/c$ space group. The metal center is hexa-coordinated with N_3O_3 donor sets, and weak coordinated interaction (Cu1-O2 0.278 9(3) nm) also exist in the $[CuL(OAc)(H_2O)]ClO_4$ unit, and the geometry around metal center can be described as a distorted octahedron. The atoms O2 and O3 occupy the axial positions (Cu1-O2, 0.278 9(3) nm and Cu1-O3, 0.245 7(3) nm), the atoms O1, N1, N2 and N3 occupy the corners of the basal plane, the angles around the copper ion within the basal plane vary from 82.26(12) to 97.49(12)° and the sum of angles spanning these five bonds is 359.76°, underscoring the flat nature of this equatorial plane.

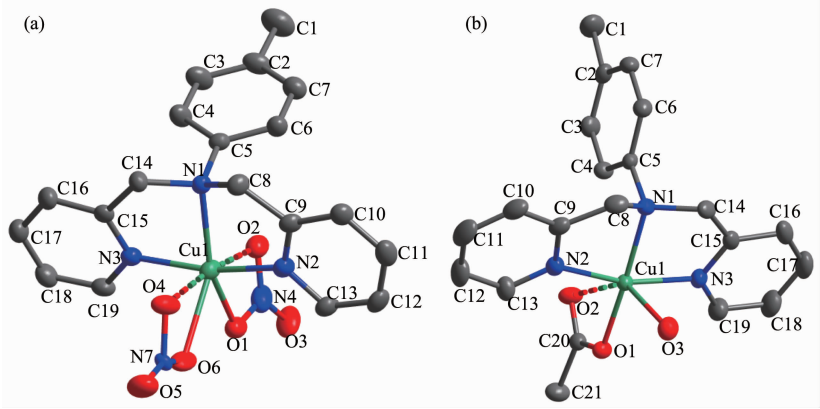

Hydrogen atoms and dissociative perchlorate ions are omitted for clarity

Fig.1 ORTEP view of the molecular structure and atom-labeling scheme of complexes **1** (a) and **2** (b) with 30% probability ellipsoid

2.2 DNA-binding and cleavage activities

2.2.1 DNA-binding study

Electronic absorption spectroscopy was an effective method in examining the binding mode and strength of the complex with CT-DNA[18]. Small molecules binding with DNA through intercalation usually result in the changes in the absorbance and shift in wavelength. The typical titration curve for **1** and **2** are shown in Fig.S1(a~b), and a plot of $(\varepsilon_a-\varepsilon_f)/(\varepsilon_b-\varepsilon_f)$ versus c_{DNA} for the titration of DNA to complex is presented in corresponding inset. As given in Table 2, the observed absorption peaks at 207 and 214 nm for complexes **1** and **2** are attributed to intraligand π-π* transition. As increasing the concentration of CT-DNA, the ligand-based bands exhibit hypochromism (For **1**, hypochromism was about 78.8% and for **2** it was 66.7%) with red shifts (10 and 7 nm for **1** and **2**, respectively) in band position, which indicates

Table 2　Absorption spectral and fluorescence spectral properties of complexes 1 and 2 bound to CT-DNA

Complex	λ_{max} / nm	Change in absorbance	$\Delta\varepsilon$ / %	Red-shift / nm	K_b / (L·mol^{-1})	K_{app} / (L·mol^{-1})
1	207	Hypochromism	78.8	10	4.21×10^4	7.13×10^5
2	214	Hypochromism	66.7	7	9.60×10^4	6.83×10^5

intercalation between the complexes and DNA[19]. To confirm the binding strength of the complexes with CT-DNA, the intrinsic binding constants K_b were calculated according to the equation[20]: $c_{DNA}/(\varepsilon_a-\varepsilon_f)=c_{DNA}/(\varepsilon_b-\varepsilon_f)+1/[K_b(\varepsilon_b-\varepsilon_f)]$, where c_{DNA} is the DNA concentration in nucleotides; ε_a is the extinction coefficient observed for the charge transfer absorption band at a given DNA concentration; ε_f is the extinction coefficient of the free complex in solution; ε_b is the extinction coefficient of the complex when fully bound to DNA. The binding constant K_b values (Table 2) follow the order: **2** (9.60×10^4 L·mol^{-1}) > **1** (4.21×10^4 L·mol^{-1}), which suggest that complex **2** has slightly stronger binding affinity than **1**. The K_b values are smaller than reported for typical classical intercalators (EB-DNA, 3.3×10^5 mol·L^{-1} in 50 mmol·L^{-1} Tris-HCl/1.0 mol·L^{-1} NaCl buffer, pH 7.5)[21], which suggests that the binding strength of the two complexes with DNA is a medium intercalative mode.

In order to further clarify the CT-DNA binding activity, fluorescence spectral measurements were carried out. No luminescence is observed for both complexes and CT-DNA at room temperature, therefore the binding activity is evaluated by the fluorescence emission intensity of EB bound to DNA as a probe. EB-DNA emits intense fluorescent due to their strong intercalation between the adjacent DNA base pairs[22], which could be quenched by the addition of another compound. The relative binding propensity of the complexes to EB-DNA studied in buffer solution (5 mmol·L^{-1} Tris-HCl/50 mmol·L^{-1} NaCl, pH=7.2) is shown in Fig.S2(a~b), and the plots of I_0/I versus $c_{complex}$ for the quenched intensity of **1** and **2** to EB-DNA are shown in the insets, respectively. Fluorescence intensities of EB-DNA at 602 nm (510 nm excitation) were measured, and the extent of reduction of the emission intensity by varying the concentration of the complexes gives a measure of the binding propensity. In the Stern-Volmer equation $I_0/I=1+Kc_Q$[23], I_0 and I represent the fluorescence intensities in the absence and presence of quencher, respectively; K is the Stern-Volmer quenching constant, and c_Q is the concentration of the quencher. The quenching plot indicates the quenching of EB bound to CT-DNA by complex is in agreement with the linear Stern-Volmer equation. In the equation $K_{EB}c_{EB}=K_{app}c_{complex}$, K_{EB} is a constant of 1.0×10^7 mol·L^{-1} (c_{EB}=2.4 μmol·L^{-1}), K_{app} is the calculated apparent binding constant values, and $c_{complex}$ is the concentration at a half reduction of the fluorescence intensity of EB. The K_{app} values (Table 2) are nearly equal and follow the order: **1** (7.13×10^5 L·mol^{-1}) > **2** (6.83×10^5 L·mol^{-1}). The apparent binding constants values are less than that of the classical intercalators and metallointercalators (1.0×10^7 L·mol^{-1})[24], indicating medium binding strength of the complexes with CT-DNA. On the whole, the result of fluorescence spectral measurements is consistent with obtained K_b values by UV spectroscopy.

2.2.2　DNA Cleavage Studies

Agarose gel electrophoresis was used to explore the supercoiled (SC) pBR322 plasmid DNA cleavage activity of the two complexes in a medium of 50 mmol·L^{-1} Tris-HCl/NaCl buffer for 4 h. In the absence of external agents, the concentration-dependent DNA cleavage activities were observed under the nearly physiological conditions (pH=7.2, 37 ℃) (Fig.S3), and both of **1** and **2** could not induce obvious DNA cleavage with the increase of concentration (10~130 μmol·L^{-1}). The ratios of SC DNA (Form Ⅰ) for complex **1** gradually reduce with the increase of concentration, while NC DNA (Form Ⅱ) doesn′t increase, which suggests that **1** partially degraded SC DNA into undetectable minor fragments[25]. When the concentration of **2** increase to 130 μmol·L^{-1}, no obvious change for the ratios of Form Ⅰ and Form Ⅱ were observed. The above suggest that **1** showed

slightly better concentration-dependent activities than **2**. The concentration-dependent DNA cleavage experidments by complex were also performed in the presence of H_2O_2 (Fig.2) and GSH (glutathione) (Fig. 3), respectively. Notably, the DNA cleavage efficiencies of both complexes exhibit remarkable enhancement. In Fig.2, at the concentration of 10 μmol·L^{-1} Cu^{2+}, both complexes are efficient cleavers of SC DNA (Form Ⅰ) and produce more than 90% of NC DNA (Form Ⅱ), which implies that H_2O_2 as a revulsant or an activator plays a vital role. When the concentration of complex increase to 40 μmol·L^{-1}, obvious LC DNA (Form Ⅲ) is produced and the ratios of which followed the order of **1** (57.3%) > **2** (31.0%). In order to further clarify the vital role of external revulsant, the GSH (glutathione) instead of H_2O_2 were added. Similarly, as shown in Fig.3 (lane 2~5), the DNA cleavage efficiencies of both complexes also exhibit remarkable increases. At the concentration of 50 μmol·L^{-1} Cu^{2+}, the DNA cleavage efficiencies (the ratios of Form Ⅲ) follow the order of **1** (61.8%) > **2** (45.2%). Both H_2O_2 and GSH showed similar behavior in DNA cleavage reactions, although H_2O_2 was slightly more active than GSH.

To further assess the cleavage rate of chemical nuclease, the kinetic parameters for complexes **1** and **2** promoted DNA cleavage were determined. The time-dependence of DNA cleavage experiments were carried out (Fig.4) under the same condition (pH=7.2, 37 ℃, c_{GSH}=250 μmol·L^{-1}, $c_{Cu^{2+}}$=10 μmol·L^{-1}). The

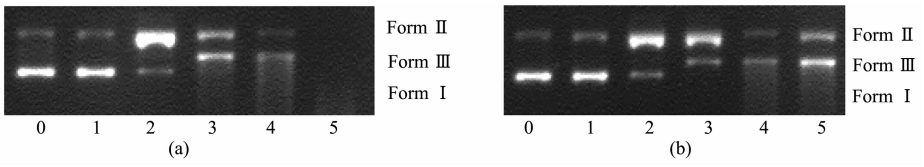

Lane 0: DNA control (4 h); lane 1: DNA+250 μmol·L^{-1} H_2O_2; lane 2~5: DNA+H_2O_2+complex (10, 40, 70, 100 μmol·L^{-1}, respectively)

Fig.2 Gel electrophoresis diagrams showing the cleavage of pBR322 DNA (0.1 μg·μL^{-1}) with complex 1 (a) and 2 (b) in Tris-HCl/NaCl buffer (pH=7.2) at 37 ℃

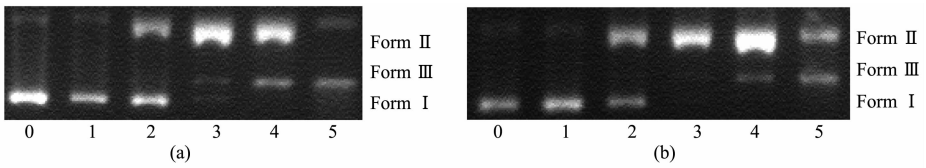

Lane 0: DNA control (4 h); lane 1: DNA+250 μmol·L^{-1} GSH; lane 2~5: DNA+GSH+complex (5, 20, 35, 50 μmol·L^{-1}, respectively)

Fig.3 Gel electrophoresis diagrams showing the cleavage of pBR322 DNA (0.1 μg·μL^{-1}) with complex **1** (a) and **2** (b) in Tris-HCl/NaCl buffer (pH=7.2) at 37 ℃

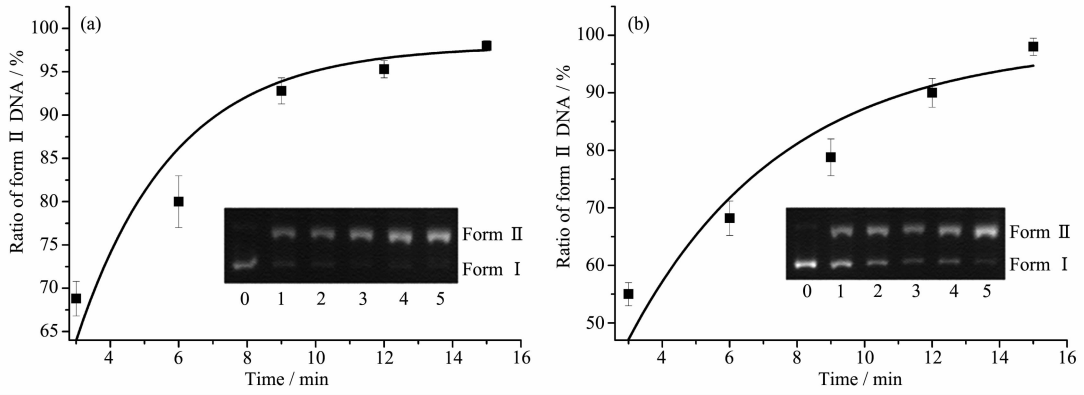

Tris-HCl/NaCl buffer (pH=7.2) at 37 ℃; Inset: lane 0: DNA control (15 min); lane 1~5: DNA+250 μmol·L^{-1} GSH+10 μmol·L^{-1} complex (3, 6, 9, 12, 15 min), respectively

Fig.4 Time-dependence of pBR322 DNA cleavage by complexes **1** (a) and **2** (b) according to the inset

ratios of Form Ⅰ gradually disappeared and Form Ⅱ increased with reaction time increase (3~15 min). More than 90% NC DNA (Form Ⅱ) was observed within 9 min for complex **1** (Fig.4a Inset) and within 15 min for complex **2** (Fig.4b Inset). The decrease of Form Ⅰ or increase of Form Ⅱ was fitted to a single exponential decay curve (pseudo-first-order kinetics) by the equation[26-27]: $y=(100-y_0)[1-\exp(-k_{obs}x)]$, where y_0 is the initial ratio of a form of DNA; y is the ratio of a specific form of DNA at time x; k_{obs} is the apparent rate constant. The reaction profile for the complex displayed approximately pseudo-first-order kinetic behavior (Fig.4(a~b)) with k_{obs} follow the order of **1** (0.35 min^{-1}) > **2** (0.22 min^{-1}), showing better than the result of the k_{obs} for copper-ATCUN complexes (0.07 and 0.14 min^{-1}) obtained by Cowan′s group[28].

In order to obtain the information about the active oxygen species (ROS) which was responsible for the DNA cleavage, the potential mechanism of DNA cleavage mediated by the complex was investigated in the presence of GSH. DNA cleavage experiments (Fig. 5) were carried out using reagents like KI as hydroxyl radical scavenger (·OH), NaN_3 as singlet oxygen ($^1O_2$) quencher, EDTA as the chelator of complex, catalase as hydrogen peroxide scavenger, and superoxide dismutase (SOD) as O_2^- radical scavenger. In Fig.5(a~b), addition of KI (lane 3) to SC DNA partly inhibited the DNA cleavage activity, which suggested the possible involvement of hydroxyl radial (·OH) as the reactive species. Also, the complexes showed partial inhibition of DNA-cleavage in the presence of the NaN_3 (lane 4), and D_2O (lane 8) enhanced the DNA cleavage [29], indicating possible involvement of singlet oxygen as the reactive species. No obvious inhibition was observed for other radical scavengers. Therefore, the data suggest the involvement of both hydroxyl radicals (·OH) and singlet oxygen ($^1O_2$) as ROS. In addition, The EDTA (lane 5), a Cu (Ⅱ)-specific chelating agent that strongly bind to Cu(Ⅱ) forming a stable complex, can efficiently inhibit DNA cleavage, indicating metal ion plays the key role in the cleavage. The addition of methyl green (lane 9), which is known to interact to DNA at major groove [30], effectively inhibited DNA cleavage by complex. The result suggests that the complex mainly has interaction with DNA through major groove.

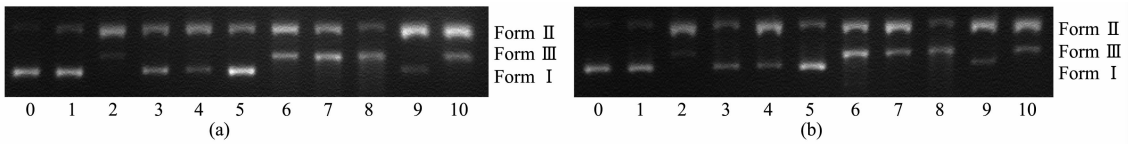

Lane 0: DNA control; lane 1: DNA+0.25 mmol·L^{-1} GSH; lane 2: DNA+0.25 mmol·L^{-1} GSH+complex; lane 3~10: DNA+0.25 mmol·L^{-1} GSH+complex+inhibitors (0.1 mol·L^{-1} KI, 0.1 mol·L^{-1} NaN_3, 0.5 mmol·L^{-1} EDTA, 0.2 U·mL^{-1} Catalase, 2 U·mL^{-1} SOD, 55% (*V*/*V*) D_2O, 0.1 mmol·L^{-1} methyl green, 0.15 μL·mL^{-1} SYBR green, respectively)

Fig.5　Cleavage of plasmid pBR322 DNA (0.1 μg·$μL^{-1}$) in presence of 20 μmol·L^{-1} complex **1** (a)~**2** (b) (0.04% DMF) and different inhibitors after 4 h incubation at 37 ℃

2.3　MTT assay

MTT (3-(4,5-dimethylthiazol-2-yl)-2,5-diphenyltetrazolium bromide) assay is a colorimetric assay based on the conversion of the yellow tetrazolium salt to purple formazan crystals by metabolically active cells, which has been done to test the ability of complexes to inhibit cell growth and induce cell death in HeLa (human cervical carcinoma), HepG-2 (human liver hepatocellular carcinoma) and SGC-7901 (human gastric carcinoma) cancer cell lines. In Table 2, both

Table 2　IC_{50} of complexes 1 and 2 obtained with different cell lines for 48 h

Complex	IC_{50} / (μmol·L^{-1})		
	HeLa	HepG-2	SGC-7901
1	> 50	40.3±3.0	35.5±2.5
2	> 50	34.2±2.3	32.4±2.0
Cisplatin	10±2.2	25±3.1	< 6.5

1 and **2** exhibit significant cytotoxic activities toward tested tumor cells and inhibit the growth of cells in a dose-dependent manner, and **2** shows slightly better antitumor effect than **1**. Complex **2** exhibits strong anti-proliferative effect on HepG-2 cells with the IC_{50} value of (34.2±2.3) μmol·L^{-1}, which is close to the cisplatin (IC_{50}=(25±3.1) μmol·L^{-1}) and probably has the potential to act as an effective metal-based anticancer drug.

3 Conclusions

Two new mononuclear Cu(Ⅱ) complexes have been synthesized and characterized. Crystal structure showed that the metal center of **1** is hepta-coordinated with N_3O_4 donor sets, existing weak coordinated interactions, and can be described as a distorted pentagonal bipyramidal. Weak coordinated interaction also exists in the crystal unit of **2** where the metal center is hexa-coordinated and the geometry can be described as a distorted octahedron. Partial intercalation and medium binding strength between the complexes and CT-DNA has been demonstrated. The DNA cleavage efficiencies of both complexes exhibit remarkable enhancement in the presence of H_2O_2 or GSH, and H_2O_2 was slightly more active than GSH. The oxidative cleavage mechanism was confirmed via a pathway involving formation of both ·OH and $^1O_2$ as ROS. The *in vitro* cytotoxicity of the complexes has been assessed by MTT on tumor cells lines (HeLa, HepG-2 and SGC-7901), both **1** and **2** exhibit significant cytotoxic activities and inhibit the proliferation of cells.

Acknowledgements: This work was supported by the National Natural Science Foundation of China (Grant No. 31171580), Scientific and Technologial Innovation Programs of Higher Education Institutions in Shanxi (Grant No.2015148), Natural Science Foundation of Shanxi (Grants No. 201601D011076, 201701D221157), Shanxi Key Research and Development Program (Grants No.201703D221008-4, 201703D221004-5), Shanxi Agricultural University youth top-notch innovative personnel support program (Grant No.201203), the PhD Research Startup Foundation of Shanxi Agricultural University (Grant No.2013YJ40), The Key Scientific Research Projects of Coal Fund in Shanxi (Grant No.FT201402-01). The Natural Science Foundation of Inner Mongolia (Grant No. 2016BS0206), and The Inner Mongolia Autonomous Region Higher Scientific Research Project (Grant No.NJZY088).

Supporting information is available at http://www.wjhxxb.cn

References:

[1] Mjos K D, Orvig C. *Chem. Rev.*, **2014**,**114**(8):4540-4563

[2] Muhammad N, Guo Z. *Curr. Opin. Chem. Biol.*, **2014**,**19**:144-153

[3] Garbutcheon-Singh K B, Grant M P, Harper B W, et al. *Curr. Top. Med. Chem.*, **2011**,**11**(5):521-542

[4] Barone G, Terenzi A, Lauria A, et al. *Coord. Chem. Rev.*, **2013**,**257**(19/20):2848-2862

[5] Deo K M, Pages B J, Ang D L, et al. *Int. J. Mol. Sci.*, **2016**, **17**(11):1818(17 pages)

[6] Zaki M, Arjmand F, Tabassum S. *Inorg. Chim. Acta*, **2016**, **444**:1-22

[7] Marloye M, Berger G, Gelbcke M, et al. *Future Med. Chem.*, **2016**,**8**(18):2263-2286

[8] Ott I, Gust R. *Arch. Pharm.*, **2007**,**340**(3):117-126

[9] Santini C, Pellei M, Gandin V, et al. *Chem. Rev.*, **2014**,**114**(1):815-862

[10]Storr T, Thompson K H, Orvig C. *Chem. Soc. Rev.*, **2006**,**35**(6):534-544

[11]Salassa L. *Eur. J. Inorg. Chem.*, **2011**(32):4931-4947

[12]Gao C Y, Ma Z Y, Zhang Y P, et al. *RSC Adv.*, **2015**,**5**(39):30768-30779

[13]Gao C Y, Qiao X, Ma Z Y, et al. *Dalton Trans.*, **2012**,**41**(39):12220-12232

[14]Zhang Y P, Ma Z Y, Gao C Y, et al. *New J. Chem.*, **2016**,**40**(9):7513-7521

[15]Sheldrick G M. *SHELXS*-97, *Program for the Solution of Crystal Structure*, University of Göttingen, Germany, **1997**.

[16]Sheldrick G M. *SHELXL*-97, *Program for the Refinement of Crystal Structure*, University of Göttingen, Germany, **1997**.

[17]ZHANG Yong-Po(张永坡), YANG Jia-Jia(杨佳佳), LÜ Jia-Yuan(吕佳苑), et al. *Chinese J. Inorg. Chem.*(无机化学学报), **2016**,**32**(12):2172-2182

[18]Marmur J. *J. Mol. Biol.*, **1961**,**3**(2):208-218

[19]Baldini M, Belicchi-Ferrari M, Bisceglie F, et al. *Inorg. Chem.*, **2004**,**43**(22):7170-7179

[20]Wolfe A, Shimer Jr G H, Meehan T. *Biochemistry*, **1987**,**26**(20):6392-6396

[21]Strothkamp K G, Strothkamp R E. *J. Chem. Educ.*, **1994**,**71**(1):77-79

[22]Meyer-Almes F J, Porschke D. *Biochemistry*, **1993**,**32**(16):4246-4253

[23]Lakowicz J R, Weber G. *Biochemistry*, **1973**,**12**(21):4171-4179

[24]Cory M, McKee D D, Kagan J, et al. *J. Am. Chem. Soc.*, **1985**,**107**(8):2528-2536

[25]Ramakrishnan S, Shakthipriya D, Suresh E, et al. *Inorg. Chem.*, **2011**,**50**(14):6458-6471

[26]Googisman J, Kirk C, Dabrowiak J C. *Biophys. Chem.*, **1997**, **69**:249-268

[27]Ordoukhanian E, Joyee G F. *J. Am. Chem. Soc.*, **2002**,**124**(42):12499-12506

[28]Jin Y, Cowan J A. *J. Am. Chem. Soc.*, **2005**,**127**(23):8408-8415

[29]Merkel P B, Kearns D R. *J. Am. Chem. Soc.*, **1972**,**94**(3):1029-1030

[30]Gibellini D, Vitone F, Schiavone P, et al. *J. Clin. Virol.*, **2004**,**29**(4):282-289